LITHOLOGY PREDICTION USING ROCK PHYSICS AND ACOUSTIC IMPEDANCE FOR RESERVOIR DISTRIBUTION IN NORTHERN PATTANI BASIN, GULF OF THAILAND

Mayura Dangprasitthiporn

Department of Geology, Faculty of Science, Chulalongkorn University, Bangkok, 10330, Thailand
Corresponding author e-mail: mayura.dang@gmail.com

Abstract

The study area lies in the northern part of the Pattani Basin, Gulf of Thailand. The reservoirs in the basin are fluvial sands. The reservoir sands are compartmentalized and show rapid lateral stratigraphic changes due to their fluvial depositional environment. Imaging of these reservoir sands is not easy by using conventional seismic data. Rock physics analysis and post-stack seismic inversion techniques were applied to map these reservoir sands. According to rock physics analysis, sands and shales have a significant contrast of P-impedance within the stratigraphic interval of Early and Middle Miocene. This contrast decreases in the Oligocene interval, and it is not easy to isolate sands based on P-impedance. Therefore, P-impedance can only discriminate sands in the upper sequences. P-velocity of clean sand and pure shale shows very small or no contrast, but density is different for these lithologies. P-velocity of shale reduces dramatically in a lacustrine section of Oligocene and locally shales have lower P-velocity than sands. Consequently, P-impedance contrast also reduces and makes it difficult to differentiate sand and shale based on P-impedance. The inversion results gave a reasonable match with P-impedance logs at well locations, and blind test results show a good match between actual and predicted P-impedance. Sand bodies were extracted by using computed thresholds of P-impedance based on rock physics cross-plots. Two types of channel belts were observed; 1) high sinuosity and narrow belts within Early Miocene and 2) large and broad channel belts in Middle Miocene. The present study concludes that post-stack P-impedance inversion can successfully map sand reservoirs and determine their connectivity.

Keywords: P-impedance, Post-stack seismic inversion, Pattani Basin

1. Introduction

The study area lies within the northern part of the Pattani Basin, Gulf of Thailand (Figure 1). The reservoirs in this basin are highly compartmentalized due to the fluvial depositional environment. The rapid lateral stratigraphic changes are a primary factor causing this compartmentalization. These results in high uncertainty in predict a reservoir sands.

Seismic data provides important information about general geology. However, the reservoir sands in the Pattani Basin are not always possible to map based on seismic amplitudes. In this study, I aimed to predict reservoir sands by applying post-stack seismic inversion technique. The post-stack seismic inversion serves as one of the tools for estimating detailed characteristics of the reservoirs (Pendrel and Van Riel, 1997). Moreover, seismic inversion can quantify the sands in the area while amplitude maps show only relative variation of lithology and it in turn gives better estimations of reservoir properties such as net pay and porosity. An additional benefit is that interpretation efficiency is greatly improved by applying inversion technique (Pendrel, 2001).

The key objectives of the present study are to evaluate different rock physics parameters such as velocity, density and P-impedance for hydrocarbon and lithology prediction by applying post-stack seismic inversion and map the distribution of reservoir sands in the Miocene interval and identify the sands that is connected.

2. Study Area

The study area lies within the northern part of Pattani Basin, Gulf of Thailand. The Pattani Basin is a Tertiary basin formed in response to extension as the result of the northward movement of the Indian plate and its collision with Eurasia to create a complex system of rift basins with half-graben geometries (Morley et al. 2011).

Morley and Racey (2011) divided the basin into five stratigraphic sequences, which contain more than 8000 m of sediments. The sequence 1, Late Eocene to Oligocene, is comprised of alluvial sediments grading into lacustrine sediments. Sequence 2 is of Early–Mid-Miocene age. Depositional environments of this sequence include fluvial, lower delta plain and intertidal. Sequence 3 is of Mid-Miocene age. This sequence associated with a transgressive phase in the basin's history, the depositional environment is fluvial/ deltaic with occasional marginal marine deposits. This was followed by fluvio-deltaic deposition environment deposited during a regression in sequence 4, in late Middle to Late Miocene age. The uppermost, sequence 5, Late Miocene–Recent age, comprises predominately transgressive marginal marine deposition.

The main reservoirs in this study area are fluvial and fluvio-deltaic sandstone within sequence 2 and sequence 3. The depth of these reservoirs varies from 1350-2200 m.

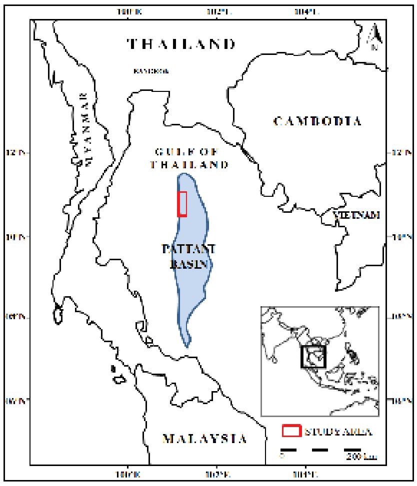

Figure 1: Study area located in the northern part of the Pattani Basin (Modified from Jardine, 1999)

3. Methodology

3.1 Rock Physics

The rock physics analysis aims to 1) determine the rock properties, which can discriminate and differentiate lithology and 2) study the acoustic impedance response to variation in lithology and fluids. Cross-plots of P-impedance (P-impedance is a product of rock density and P-wave velocity), density and velocity against shale volume were created to observe the response of these rock physics parameters for sand and shale. Moreover, the cross-plots were analyzed as a function of depth to check the depth dependency of the rock physics parameters such as P-impedance, density and velocity. The logs were up-scaled to the seismic data, to compare the impedance inversion with well data. Cross-plot analysis was performed for different depth and stratigraphic intervals. The sand reservoir defined by using shale volume cut-off is less than 30% whereas the cut-off for water saturation is defined as 65%.

3.2 Post-stack Seismic Inversion

In this study, the seismic data volume was inverted into acoustic impedance volume by using the model-based inversion technique. The first step is initial model building. The seismic data is band limited and does not include very low frequencies. Low frequencies were added in the initial model by using well logs. Three horizons (TopSeq3, TopSeq2 and TopSeq1) were used structurally to guide the interpolation of P-impedance within the initial model. After building the initial model, model-based inversion technique was applied on it and inversion analysis would be done.

4. Results

4.1 Rock physics

Sands are characterized by low velocity and density. Whereas, shales show comparatively higher velocity and density. Consequently, the acoustic impedance in the sands is lower than the shales.

The results of cross-plot analysis of different stratigraphic show that P-impedance values of the sands and shales increases with depth. In sequence 3 (Lower Middle Miocene), sands have lower P-impedance and can be isolated from the shales based on the P-impedance contrast at a cutoff value of 7100 g/cc*m/s (Figure 2a). Although mostly shales have higher P-impedance yet there are some points on the cross-plot that show lower values in the range of P-impedance of the sands. In sequence 2 (Lower Miocene), sands also have lower P-impedance. The cutoff value of sand is define as 8000 g/cc*m/s (Figure 2b). Sequence 1 (Oligocene), P-impedance of the sands and the shales is overlapping partially (Figure 2c). Therefore sands and shale cannot be separated always based on P-impedance. However, Fluid component (hydrocarbon/water-saturated sandstone) cannot be distinguished by using P-impedance contrast as shown in Figure 2. The P-impedance of hydrocarbon saturated sands and water-wet sands are the same.

Figure 3 shows cross-plot of P-impedance with respect to shale volume color coded by total porosity (PHIT). It reveals that P-impedance can indicate the high porous sand zones. The high porosity of sands has relatively lower P-impedance.

The cross-plot analysis of P-impedance and shale volume suggests that the P-impedance contrast between sands and shales is significant in sequence 3 and 2. However, P-impedance of sand and shale is partially overlapped within the sequence 1. Consequently, post-stack seismic inversion of P-impedance will be suitable to differentiate sands from shales in sequence 3 and sequence 2 whereas it is not always possible to distinguish lithologies in sequence 1. Moreover, P-impedance can also delineate high porosity sands.

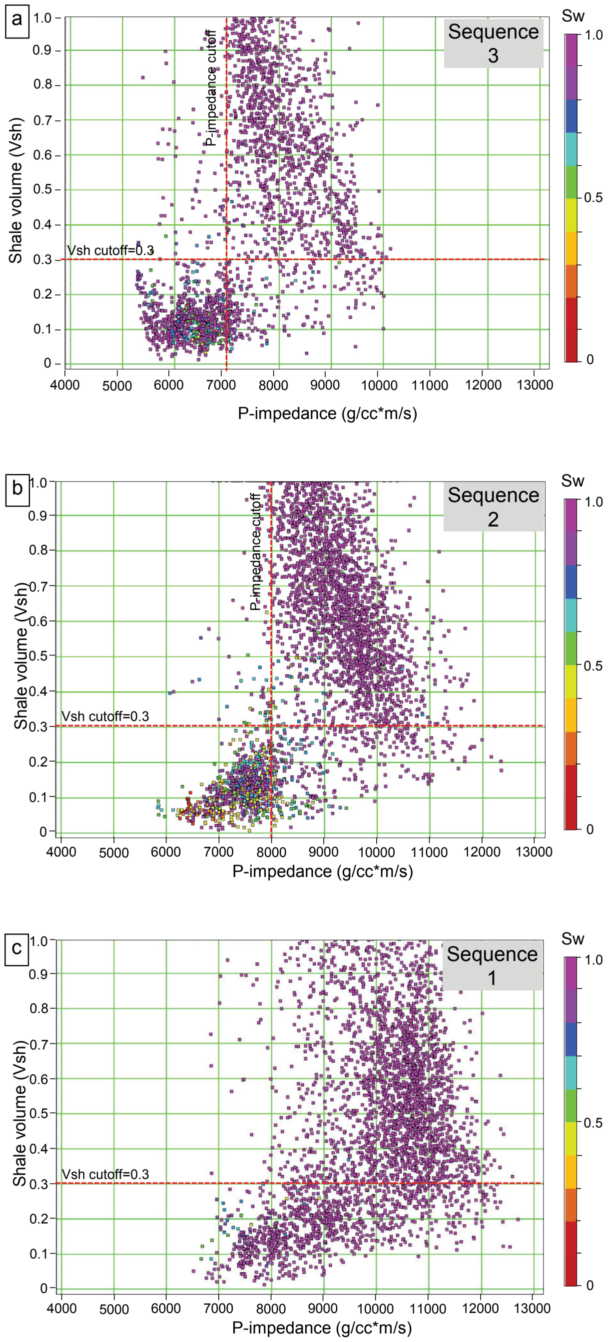

Figure 2: Cross-plot of P-impedance and shale volume color coded by Sw for a) sequence 3, b) Sequence 2, and c) Sequence1 shows P-impedance can discriminate sands and shales for sequence 3 and 2 but in sequence 1, P-impedance of sands and shales are overlapping. It is difficult to isolate all sands from shale. However, hydrocarbon sands cannot be separated based on P-impedance values for all depth.

Cross-plots of density and shale volume (Figure 4a) show that sands have a lower density than shales. The density shows significant contrast for all depth intervals. This suggests that density is more effective to discriminate lithology.

P-velocity increases with depth as shown in Figure 4b. Clean sands have low P-velocity. P-velocity increase as shale percentage increases. This increase in P-velocity was observed till 30% shale content and beyond 30% shale content P-velocity decreased.

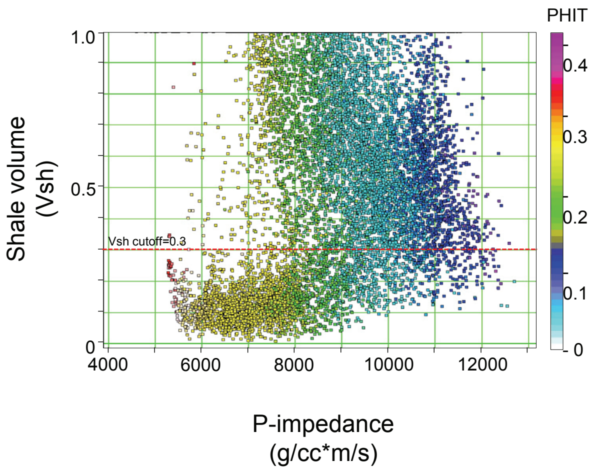

Figure 3: Cross-plot of P-impedance with respect to shale volume and color coded by PHIT. High porosity sands have low P-impedance.

Furthermore, density, P-velocity and P-impedance were plotted against depth to observe the trend of these rock physics parameters against depth (Figure 5). Figure 5a shows the significant contrast of density between sands and shales within all depth intervals, but the contrast gets less as depth increase. Whereas cross-plot of velocity and depth (Figure 5b) shows that there is less contrast between sands and shale. However, some shales show extremely low values of P-velocity within sequence 1. Similarly, cross-plot of P-impedance and depth (Figure 5c) reveals those sands have lower P-impedance than shales and there is significant P-impedance contrast in the shallow section but in sequence 1 there is less contrast. Thus, P-impedance values in sequence 1 cannot isolate sands from shales due to 1) less density contrast 2) very low P-velocity of shales.

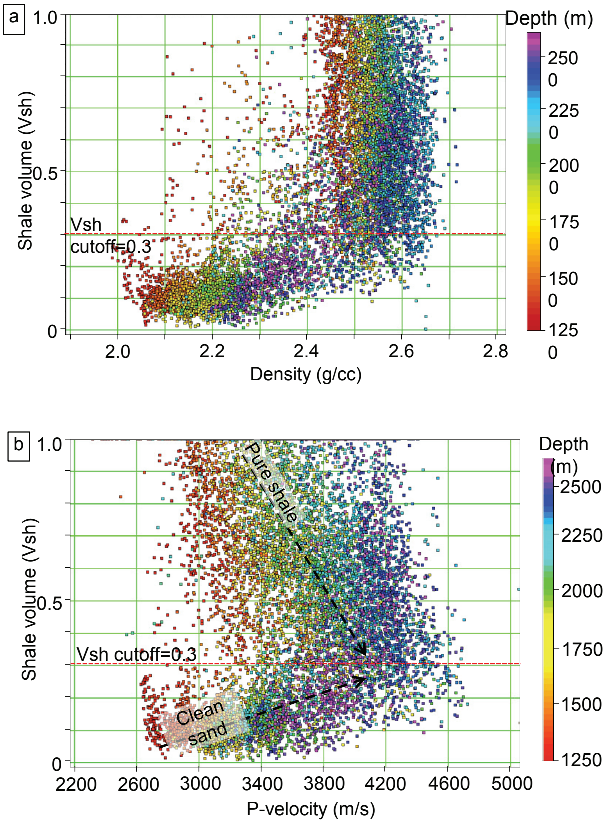

Figure 4: a) Cross-plot of density respect to shale volume. Density of sands are lower than shales for all depths. b) Cross-plot of P-velocity with respect to shale volume indicated that P-velocity of sands and shales are in the same range.

Some shales within the sequence 1 show very low P-velocity and low density. These shales have P-velocity lower than the sands. The gamma ray values are very high within these shales (>200API). Ying Li at al. (2014) studied a rock physics model for the characterization of organic shale. They explained that the increase of kerogen content might cause a decrease in velocities and density. Meyer and Nederlof (1984) researched source rock characteristics on a combination of logs that showed a lower density and increasing sonic transit time than other sediments of equal compaction and comparable mineralogy. Therefore, very low P-impedance shales can be interpreted as organic rich shale. These low P-impedence shales are located within the lacustrine sequence.

In summary, the rock physics analyses; P-impedance inversion can only detect sands

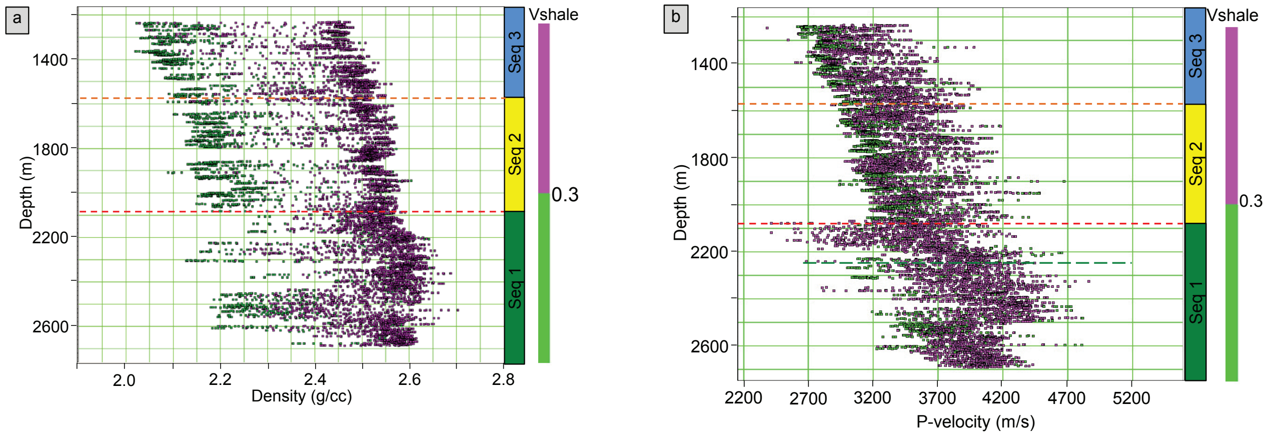

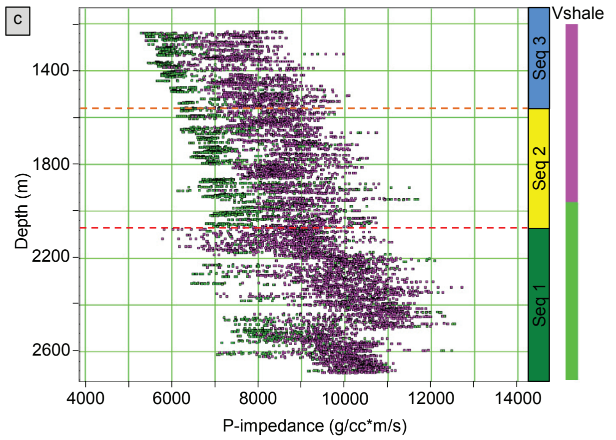

Figure 5: Figure 8 Plot of a) density, b) P-velocity and c) P-impedance versus depth color coded by shale volume.

in sequence 3 and 2 (shallow and middle sections). While the inversion method capable of solving for density would be more efficient for discriminating sand from shale for all depth.

4.2 Post-stack Seismic Inversion

The wavelet was extracted along well for four wells. It used for well to seismic tie and inversion process. The dominant frequency is about 32 Hz.

The initial guess model was built by interpolating the P-impedance data of four well and structurally controlled by three horizons (TopSeq3, TopSeq2 and TopSeq1). The values of P-impedance were interpolated along the horizons. The model was created for interval 900-2200 ms, which covers the available well log data of four wells. Low frequencies below 10 Hz were not present in the seismic data, so low frequencies were added from well log data.

Inversion Analysis

The comparison of extracted pseudo logs from P-impedance inversion volume at four well locations show a reasonable match with original P-impedance and the RMS error range from 430 to 540 with a high value of correlation coefficient (0.90).

Comparison of Inverted Volume to Original Logs.

A good agreement exists between P-impedance of logs and the P-impedance derived from the inverted volume in sequence 3 and sequence 2 (Figure 6a and 6b). The inverted volume does not show a good match in sequence 1 but I could observe that some sands can be detected on inverted P-impedance (Figure 6c). It also supports the results of rock physics. According to the rock physics analysis, because of lower values of P-impedance of shale within this stratigraphic interval I can only partially differentiate sands and shales based on P-impedance within this sequence 1. These low P-impedance values in shale may be due the presence of organic material. Moreover, sands within this interval are relatively thin and could not be resolved on the seismic data.

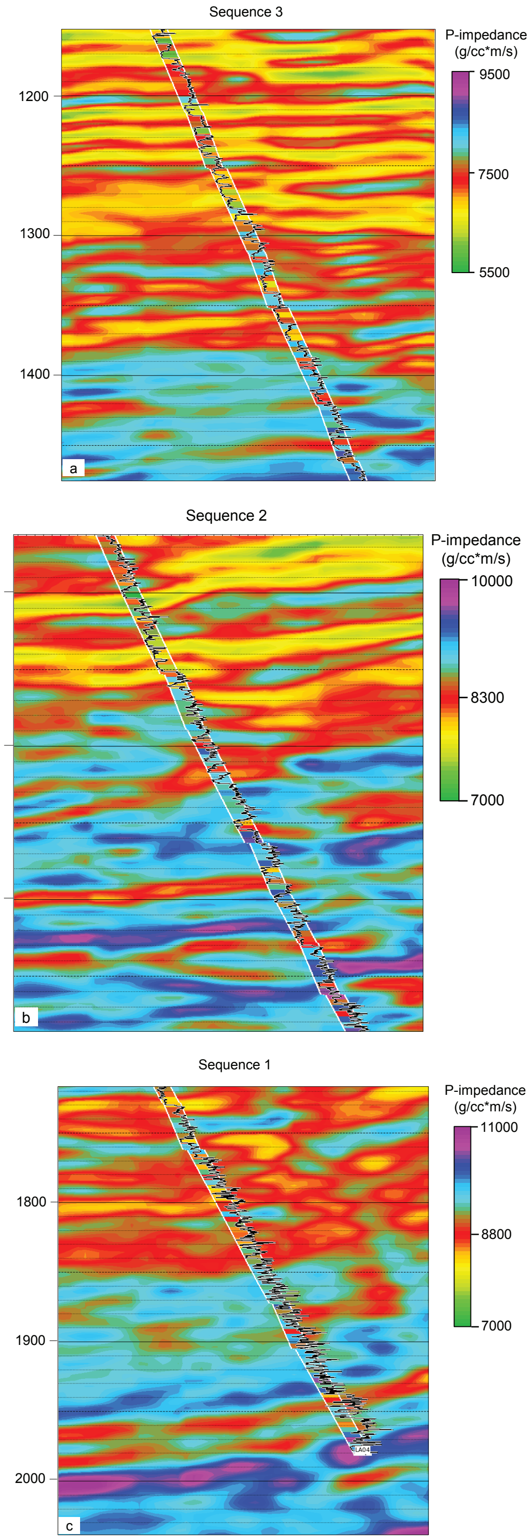

Figure 6: Cross-section of inverted P-impedance section along LA04 well. GR and original P-impedance logs are displayed for the comparison within a) sequence 3, b) sequence 2 and c) sequence 1. They show reasonable match between inverted volume and original P-impedance of logs for sequence 3 and 2 but it show poor prediction for sequence 1.

Blind Test

Blind Test analysis was performed for the wells, where not used in the inversion process. The following sections (Figure 7) show the comparison of inverted P-impedance and GR log. I used two wells for the blind test (LA05 and LAWA-07). Both of these wells show a reasonable match with GR log. Low GR values correspond to low P-impedance values on the inverted section. The results show a good match in sequence 3 and 2 but not always reasonable match for sequence 1.

Interpretation of Sand Distribution

The low values of P-impedance were extracted along horizon slice to image the lateral distribution of sands within sequences 3 and 2. As discussed in the rock physics analysis, sands have values of 7100 g/cc*m/s and 8000 g/cc*m/s in sequence 3 and sequence 2 respectively. These mentioned values are used to differentiate sands from shales within the respective sequence.

Figures 8 present the map view of P-impedance image with line-drawing interpretations of the recognizable, geologically meaningful patterns of sand distribution. Figure 8a represents the map view impedance image for sands within sequence 3. The image reveals that sands are very broad with low sinuosity. The map of TopSeq2 +116ms represents the upper part of sequence 2 (Figure 8b), illustrates high sinuosity like channel feature as shown in line-draw interpretation. The lower part of sequence 2 has narrower channels with relatively high sinuosity (Figure 8c). These channels like feature are orientated in N-NW to S-SE direction.

5. Discussions

5.1 Sand Connectivity and Reservoir Implication

The distribution of sand bodies and their connectivity are critical for accurate reservoir models and future exploitation programs. I used P-impedance volume to check the connectivity of the sands. Figure 9 shows different sand bodies within the sequence 2. To obtain this map; connected sands greater than minimum defined

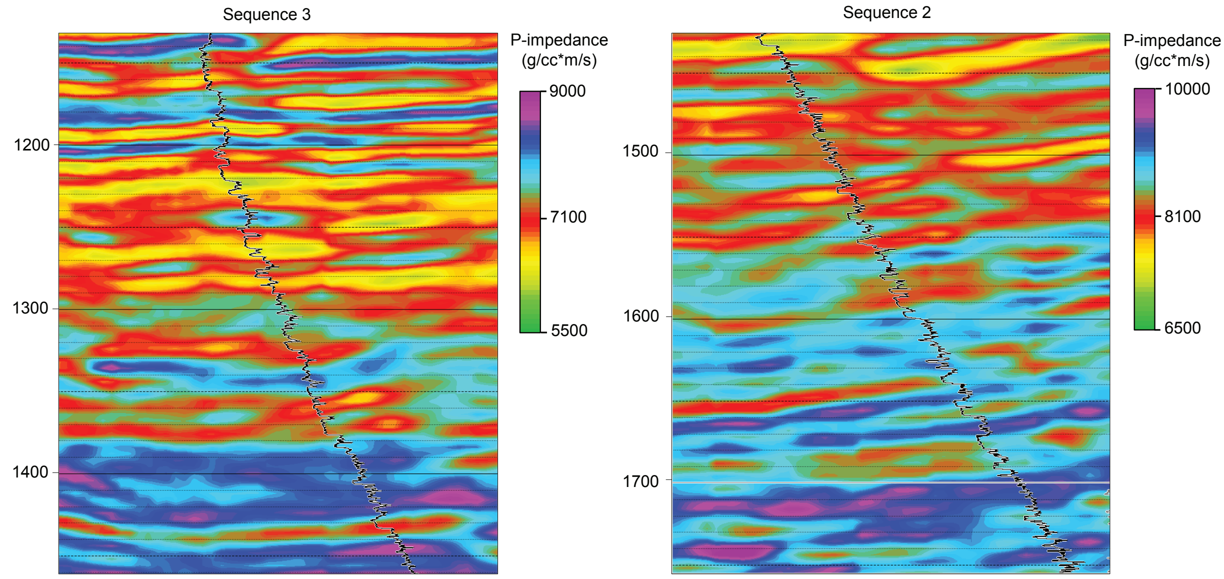

Figure 7: The results of blind test wells on cross-sections along well LAWA-07 in sequence 3 and 2 with gamma-ray log displayed. It shows reasonable match with gamma ray log in both sequence.

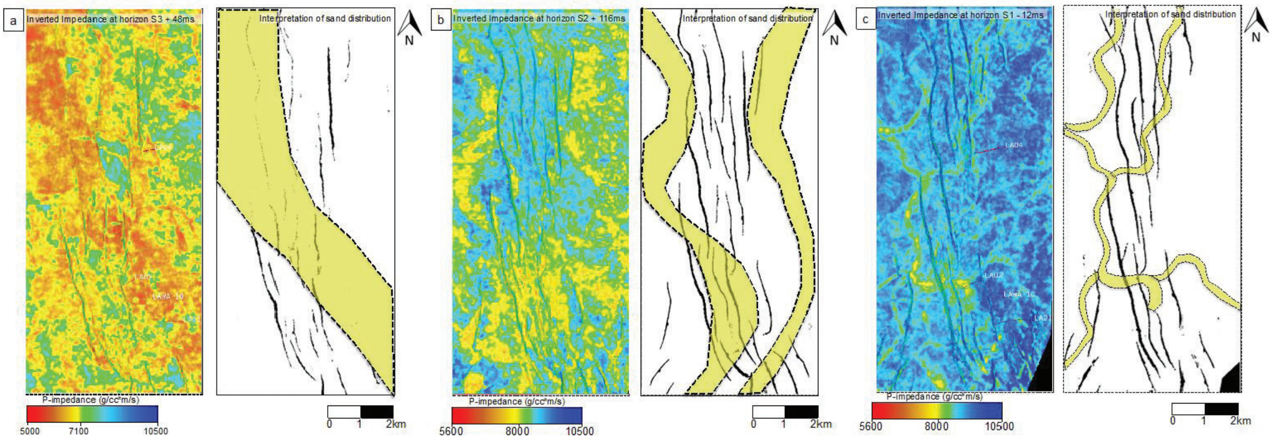

Figure 8: Horizon slices of inverted impedance data for a) sequence 3, b) upper part of sequence 2 and c) lower part of sequence 2 with interpreted draw-line of the recognizable, geologically meaningful patterns of sand distribution.

size of voxels threshold were assigned the same color. Sand body connectivity is associated with several factors:

- The depositional styles of sediment feature of lateral dimensions.
- Sand bodies may be deposited at different, unconnected stratigraphic levels within that interval (stacked sand bodies).
- Faults break sand connectivity.
- Lateral variation in quality of sands.
- Juxtaposition of sands across faults.

The predicted distribution of sands shows that sands are scattered in a complex pattern, and their connectivity varies in different stratigraphic succession.

5.2 Depositional Environments and Tectonic Control on Sedimentation

According to Morley and Racey (2011), a syn-rift phase occurred in Eocene to Oligocene, syn-rift to post-rift transition phase from Early Miocene to Middle Miocene and regional post-rift subsidence phase in late Middle Miocene-Recent. During the latest Oligocene or earliest Miocene, a profound change in sedimentation is seen in the eastern Gulf of Thailand. The lacustrine sediments became swamped by the deposition of coarse to fine-grained sediment. In the study area, the analysis of P-impedance horizon slices reveal that the lower part of sequence 2 has relatively narrower and higher sinuosity channels than the upper part of this sequence, while broad style sands are commonly found in sequence 3. The narrower sands in the lower part can be interpreted as the result of lacustrine to fluvial transition. Then, followed by well-developed fluvial sands in the upper section of sequence 2 and 3.

In this study area, Syn-rift section can be observed easily in sequence 1 by showing thickening to eastward. Sequence 2 a bit of thickening was observed. Channel sands are narrow and aligned mostly north-south in the lower part of sequence 2. The alignment is in agreement with fault orientation. Therefore, in the early syn-rift to post-rift transition sedimentation probably controlled by faults. However, there is insufficient evidence on a vertical seismic section to observe thickening of sands along the fault due to limited seismic resolution.

6. Conclusions

Rock physics analysis and post-stack seismic inversion were applied to map the Miocene reservoirs in the northern part of the Pattani Basin, Gulf of Thailand. The key findings and conclusions are summarized below;

- According to rock physics, P-impedance data volumes can clearly differentiate sand and shale in sequence 3 (Middle Miocene) and sequence 2 (Early Miocene), but in sequence 1 (Oligocene) this differentiation is not always possible. However, P-impedance cannot identify hydrocarbon-saturated sands in all three sequences.

- P-impedance data volume can be used to delineate high porosity sands. High porosity sands have relatively lower P-impedance.

- P-impedance data volumes have limited lithology discrimination capability in sequence 1 (Oligocene). Because P-impedance values of shales within this interval are very low due to the presence of organic material. It makes values

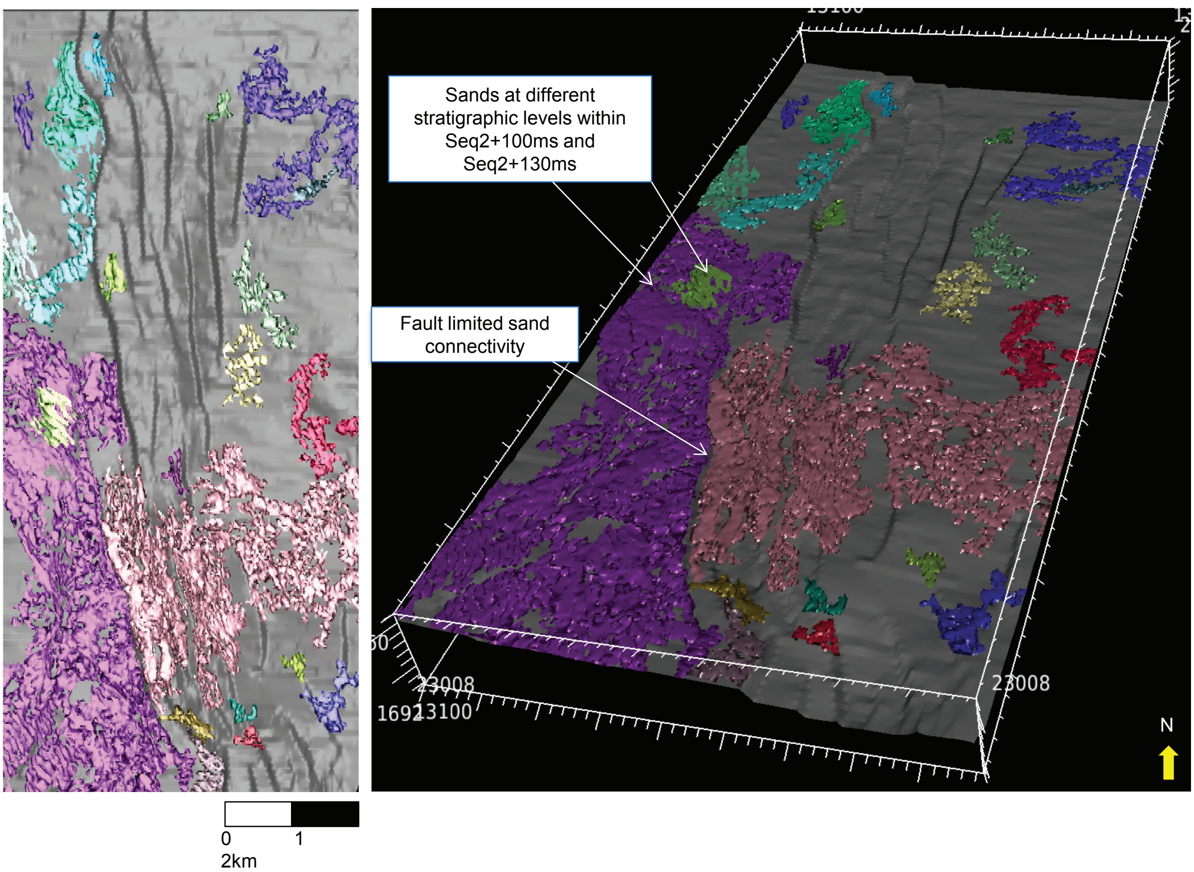

Figure 9: Map views display the extent of connectivity of sand bodies within sequence 2 (between Seq2-100ms to Seq2-130ms horizon).

sands in this interval is generally less, that also makes the prediction difficult.

- Density can discriminate sands from shales for all depths. Sands show lower values of density as compared to the shales. The density may also be useful for lithology discrimination.

- P-velocity of clean sands and pure shales are in the same range for all stratigraphic levels. Therefore, P-velocity cannot be used to differentiate sand and shale.

- The contrast of P-impedance, density and P-velocity for sand and shale decreases with depth.

- The blind test indicated a reasonable match, low GR correspond to low values of predicted P-impedance through seismic inversion for sequence 3 and 2.

- Computed cutoff values derived from rock physics for sands in sequence 2 and sequence 3 successfully isolated sand bodies in these stratigraphic intervals.

- The extracted sand bodies are of two styles 1) high sinuosity and narrow channel belts are within sequence 2 and 2) broad channel belts are within sequence 3. The narrow channels may be due to fault-controlled sedimentation in early phase of syn-rift to post-rift transition.

- Connectivity of sand bodies was determined. This information will be useful for future exploration and field development programs.

7. Acknowledgement

I would like to thank my university supervisor Dr. Mirza Naseer Ahmad, for his excellent guidance, support and providing me with an excellent atmosphere for doing research, and also my professors. My sincere thanks also goes to Chevron Thailand Exploration and Production, Ltd. for the use of their data including wireline log data and seismic data. I am thankful to my company supervisors; Mr. Lance Brunsvold, and Mr. Ken Werner for financial supporting during my graduated study. I appreciate Chevron Thailand Exploration and Production Ltd. And Petroleum Geoscience Program staffs for precious technical support throughout the year.

8. References

Cooke, D. A. and Schneider, W.A., 1983, Generalized linear inversion of reflection seismic data: Geophysics, v. 48, p. 665-676.

Jardine, E., 1997, Dual Petroleum Systems Governing The Prolific Pattani Basin Offshore Thailand: Proceedings of the Petroleum Systems of SE Asia and Australasia Conference, May 1997, p. 351-363.

Li Y, Guo ZQ, Liu C, et al., 2015, A rock physics model for the characterization of organic-rich shale from elastic properties, Petroleum Science, v. 12, issue 2, p. 264-272.

Meyer, B.L., and Nederlof, M.H., 1984, Identification of Source Rocks on Wireline Logs by Density/Resistivity and Sonic Transit Time/Resistivity Crossplots: The American Association of Petrleum Geologist Bulletim, v.68, no.2, p. 121-129.

Morley, C.K., and Racey, A., 2011, Tertiary stratigraphy, in M.F. Ridd, A.J. Barber, and M.J. Crow, eds., The geology of Thailand: Geological Society of London, p. 223-271.

Morley, C.K., Charusiri, P., Watkinson I.M., 2011, Structural geology of Thailand during the Cenozoic, in M.F. Ridd, A.J. Barber, and M.J. Crow, eds., The geology of Thailand: Geological Society of London, p. 273-334.

Pendrel, J.V., 2001, Seismic inversion-the best tool for reservoir characterization: Canadian Society of Exploration Geophysicists Recorder, v. 26, p. 16-23.

Racey, A., 2011, Petroleum geology, in M.F. Rid, A.J. Barber, and M.J. Crow, eds., The geology of Thailand: Geological Society of London, p. 351-392.

Russell, B. and Hampson, D., 1991, Comparison of Post-stack Seismic Inversion Methods, SEG Expanded Abstracts, 10, 876-878.